Environmental Research Letters

CrossMark

OPEN ACCESS

RECEIVED
17 April 2015

REVISED
15 June 2015

ACCEPTED FOR PUBLICATION
24 July 2015

PUBLISHED
8 September 2015

Content from this work may be used under the terms of the Creative Commons Attribution 3.0 licence.

Any further distribution of this work must maintain attribution to the author(s) and the title of the work, journal citation and DOI.

LETTER

Identification of two distinct fire regimes in Southern California: implications for economic impact and future change

Yufang Jin[1,2], **Michael L Goulden**[2], **Nicolas Faivre**[2], **Sander Veraverbeke**[2], **Fengpeng Sun**[3], **Alex Hall**[3], **Michael S Hand**[4], **Simon Hook**[5] **and James T Randerson**[2]

[1] Department of Land, Air, and Water Resources, University of California, Davis, CA, USA
[2] Department of Earth System Science, University of California, Irvine, CA, USA
[3] Department of Atmospheric and Oceanic Sciences, University of California, Los Angeles, CA, USA
[4] USDA Forest Service, Rocky Mountain Research Station, Missoula, MT, USA
[5] Jet Propulsion Laboratory, California Institute of Technology, Pasadena, CA, USA

E-mail: yujin@ucdavis.edu

Keywords: fire regime, economic impact, fuel management, climate change, Santa Ana winds

Supplementary material for this article is available online

Abstract

The area burned by Southern California wildfires has increased in recent decades, with implications for human health, infrastructure, and ecosystem management. Meteorology and fuel structure are universally recognized controllers of wildfire, but their relative importance, and hence the efficacy of abatement and suppression efforts, remains controversial. Southern California's wildfires can be partitioned by meteorology: fires typically occur either during Santa Ana winds (SA fires) in October through April, or warm and dry periods in June through September (non-SA fires). Previous work has not quantitatively distinguished between these fire regimes when assessing economic impacts or climate change influence. Here we separate five decades of fire perimeters into those coinciding with and without SA winds. The two fire types contributed almost equally to burned area, yet SA fires were responsible for 80% of cumulative 1990–2009 economic losses ($3.1 Billion). The damage disparity was driven by fire characteristics: SA fires spread three times faster, occurred closer to urban areas, and burned into areas with greater housing values. Non-SA fires were comparatively more sensitive to age-dependent fuels, often occurred in higher elevation forests, lasted for extended periods, and accounted for 70% of total suppression costs. An improved distinction of fire type has implications for future projections and management. The area burned in non-SA fires is projected to increase 77% (±43%) by the mid-21st century with warmer and drier summers, and the SA area burned is projected to increase 64% (±76%), underscoring the need to evaluate the allocation and effectiveness of suppression investments.

1. Introduction

Southern California's Mediterranean climate, extensive wildland-urban interface, rugged terrain, and shrub-dominated landscape fosters frequent and severe wildfire, and leads to deterrence, suppression, and damage costs that are among the highest in the United States (Keeley *et al* 2009, Moritz *et al* 2010). The impact of wildfire on Southern California has increased in recent decades, with extensive areas burned in 2003, 2007, and 2009 (Jin *et al* 2014); this impact is expected to increase further with climate change, population growth, and expanding development (Westerling *et al* 2006, 2011). Disagreement remains regarding about the relative importance of fuel accumulation versus meteorology in regulating Southern California's fire regime; this disagreement contributes to uncertainty over the effectiveness of fuel abatement and fire suppression (Minnich 1983, Conard and Weise 1998, Keeley *et al* 1999, Batllori *et al* 2013).

Southern California's climate fosters two distinct types of wildfire: rapidly expanding, wind-driven Santa Ana (SA) fires that occur mostly in September

© 2015 IOP Publishing Ltd

through December (Hughes and Hall 2010, Moritz *et al* 2010), and non-SA fires that coincide with hot and dry weather mostly in June through September (figure S1). Analyses of controls on past fire and projections of future fire have typically lumped these two types together, or have emphasized just one (Minnich 1983, Keeley *et al* 1999, Westerling and Bryant 2008, Westerling *et al* 2011). We recently developed an approach that uses spatially explicit fire records (California Department of Foresty and Fire Protection 2013) and high resolution meteorological information since 1959 to classify fires into those coinciding with SA conditions and those that do not (Jin *et al* 2014). We found that the two types of fire contributed equally to regional burned area but occurred in distinct locations (Jin *et al* 2014). SA fires were concentrated in high-wind corridors and coastal areas; many of these locations burned repeatedly during the last 50 years (figure 1, table S1). Non-SA fires typically occurred in more remote inland areas, and the majority of these locations burned just once during the past 50 years, though a few areas along heavy traffic corridors and with relatively strong summer winds burned more frequently (Jin *et al* 2014).

Southern California has a population of about 22 million people. The region includes the cities of Los Angeles and San Diego, along with numerous suburban communities, extensive undeveloped land, and four National Forests (figure 1). Most people live at lower elevations and near the coast, with communities adjacent to fire-prone areas varying widely in housing wealth (figure 1) and other economic indicators. Developing effective mitigation and adaptation strategies for wildfire requires detailed information about the influence of climate change on local meteorology and ecosystem processes. In this context, our partitioning approach creates an opportunity to improve several aspects of our understanding of regional fire dynamics in Southern California. Our specific study objectives are to (1) understand how interaction between fuels and other environmental drivers contribute to differences in fire behavior for SA and non-SA fires, (2) assess how differences in fire behavior for the two fire types influence economic damages and suppression costs, and (3) predict how SA and non-SA fires will change by the mid-21st century as a consequence of climate change. Compared with earlier work, explicit consideration of the different meteorological controls on the two different fire types may enable a more rigorous assessment of future change and may provide a blueprint for the design of improved fire projections in other areas.

2. Data and methods

Our study domain encompassed seven counties in Southern California: Santa Barbara, Ventura, Los Angeles, San Bernardino, Orange, Riverside, and San Diego (figures 1 and S1). We assembled an array of datasets to analyze the location, timing, and behavior of fires, associated structural loss and direct fire-fighting costs, possible environmental drivers including weather, vegetation, topography, and human variables, and to predict future changes from climate warming.

2.1. Fire, environmental, and economic data

We used fire perimeter data from the California Department of Forestry and Fire Protection's Fire and Resource Assessment Program (FRAP) (California Department of Foresty and Fire Protection, 2013) to identify the timing and location of wildfires during 1959–2009; data back to 1900 were also used to estimate stand age. Fires were classified into SA and non-SA fires, based on their coincidence with SA and non-SA periods, following the approach described in previous work (Hughes and Hall 2010, Jin *et al* 2014). The SA occurrence and the associated meteorological characteristics were quantified with a 6 km resolution climate dataset during 1959–2009 (Jin *et al* 2014), generated from a dynamical downscaling of the European Centre for Medium-Range Weather Forecasts reanalysis data (ERA-40) from 1959 to 2001 (Uppala *et al* 2005) using the Mesoscale Model version 5 (MM5). The North American Regional Reanalysis (NARR) (Mesinger *et al* 2006) was used to extend the time series through 2009. For each individual fire polygon, weather during the first two days of the fire was extracted from the downscaled climate data as well as monthly mean temperature, precipitation and relative humidity (RH) from the Parameter-elevation Regressions on Independent Slopes Mode project (Daly *et al* 2008) for the month spanning each fire event, along with biophysical and human variables.

We examined fire behavior, including fire intensity, progression and duration, for fires that occurred during 2002–2009 using NASA's MODerate resolution Imaging Spectroradiometer (MODIS) satellite data from Terra and Aqua satellites. Active fire pixels (based on the thermal anomalies) were detected four times daily by MODIS on Terra at 10:30 am and 10:30 pm, and on Aqua at 1:30 pm and 1:30 am (local time) with a nadir resolution of approximately 1 km. We used the Global Monthly Fire Location Product (MCD14ML) in our analysis, selecting only high quality detections for our analysis (Giglio *et al* 2003, 2013). The association of active fires to individual FRAP fires was based on the location and time of each fire detection. We also used MCD14ML fire radiative power (FRP), as a measure of intensity (Giglio *et al* 2013).

We compiled property loss data from California Fire Incident information and other sources. These data included the number of structures destroyed, structures damaged, and fatalities. Fire suppression costs were obtained for federal lands (1995–2009) from the USFS and for other lands from FRAP (Gebert

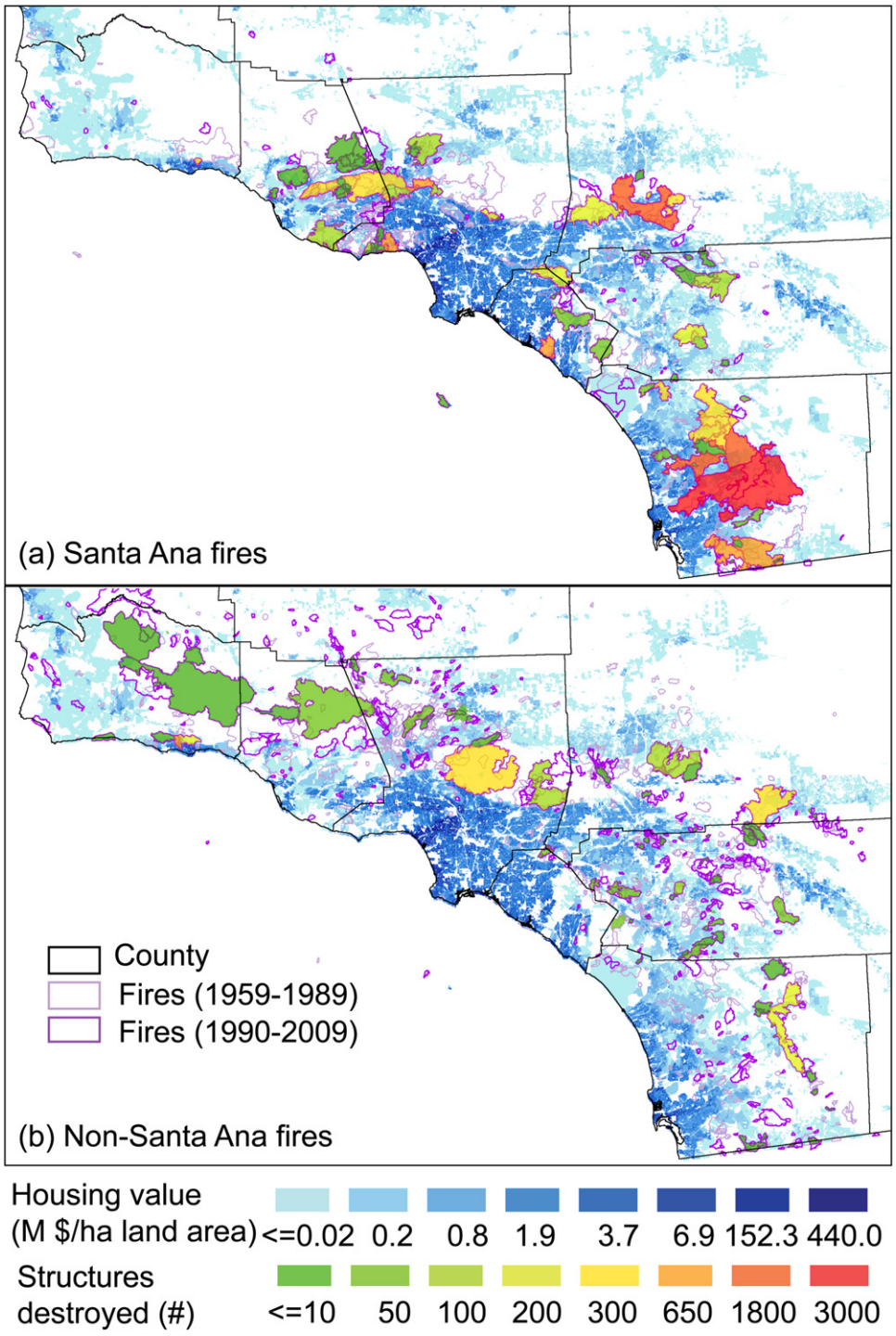

Figure 1. Patterns of structure loss during 1990–2009. Santa Ana (SA) and non-Santa Ana fire perimeters during 1959–2009 superimposed on housing value. Fires with structure loss are shaded, with colors showing total number of structures destroyed during 1990–2009. Light purple polygons represent fires occurring prior to 1990, and dark purple after 1990. Fire perimeters were obtained from California Department of Forestry and Fire Protection's Fire and Resource Assessment Program, and separated in to SA and non-SA fire types using the approach described in the methods. Housing value was estimated from Census 2000 housing density and median house prices.

et al 2007). The USFS Rocky Mountain Research Station created and maintains a fire suppression cost database for large fires reported in the Forest Service's fire occurrence database and the National Interagency Fire Management Integrated Database (Gebert *et al* 2007). Population, housing units, and median housing value statistics were obtained from the US Census Bureau's block and block-group data for 2000 to calculate the population and structures at risk within each individual fire polygon during 1990–2009. Roads information, including highways, local roads and vehicle trails, were extracted from the Census Bureau's TIGER road data (US Census 2000).

We obtained the 3 arc-second digital elevation model from the United States Geological Survey National Elevation Dataset to calculate the slope and aspect of individual fires and the location of ridgelines. Land cover types from the CalFire Multisource Land Cover dataset (California Department of Foresty and Fire Protection 2013) were used to identify possible land cover barriers for fire spread, including agriculture, urban, water, desert, and barren.

2.2. Fire behavior analysis

We estimated the fire spread rate and direction for each individual large fire based on the timing and location of MODIS active fires (Giglio *et al* 2013) The first set of detected active fire points (more than 3 counts) within the FRAP fire polygon was used to estimate a convex hull, including parameters describing the length of major and minor axis and the location of the centroid. Similarly, the convex hulls and the associated geometrical properties were derived for each fire progression time step. The mean fire spread rate was calculated as the difference between the first and final major axis divided by the time difference between the first detection time and the detection time for the 95% percentile of all fire counts within the final fire polygon. The prevailing fire progression direction was derived from the vector connecting the first to the final centroid. The spread rate with units of area was separately calculated as the area difference divided by the time difference. This estimate of fire spread rate is likely conservative given the relatively long time interval between successive Aqua and Terra overpasses, although the presence of unburned islands within some fire perimeters may contribute to additional uncertainties. To test the assumption that unburned islands (or regions with very low severity burns) did not considerably influence our spread rate calculation, we overlaid the FRAP fire perimeters on MODIS burned area product at 500 m resolution (MCD64A1) (Giglio *et al* 2009) during 2003–2009 for all fires greater than 500 acres (Figure S2). We found that unburned islands or very low severity burns accounted for a small fraction (12.6%) of the total area within the FRAP fire polygons.

Statistics were then summarized for the SA and non-SA fires, for different overpass time intervals, and stand age groups, separately. Fires smaller than 2500 ha were not included for fire behavior analysis. Fires with less than a total of 6 active fire counts detected by MODIS Terra and Aqua also were excluded because of the difficultly in deriving meaningful fire spread rates. 30 SA fires and 26 non-SA fires met these selection criteria during 2002–2009.

The FRP in the Level 2 active fire data (MCD14) was converted to fire intensity in units of W m^{-2} of ground area, by adjusting the pixel area calculated as the product of the along-scan and along-track pixel dimensions (Giglio *et al* 2013). Day- and night-time FRPs were aggregated and averaged for all pixels within the each perimeter during a given time interval, and subsequently averaged for the two different fire types.

2.3. Analysis of fuel control on fire probability and growth

We used year since fire from the FRAP fire history database as a proxy for stand age to analyze the association between fire probability and stand age for SA and non-SA fires, since the majority of wildfires in southern California are crown fires and only 1.2% of the area burned occurred within urban land cover classes. Fire probability was calculated as the percent area burned for each set of 20 year age intervals, divided by total available area within the same age interval. Only areas with at least one fire since 1959 were included in our analysis.

We also quantified the role of various barriers such as non-flammable land cover, recent burns, roads, and ridgelines in limiting the fire spread by analyzing the spatial correspondence between final burn perimeter and the position of barriers. Urban, agriculture, ocean/lake, deserts, and barren classes were considered as potential barriers and were treated equally in this study. For each 100 m pixel along the fire perimeter, a 1.1 × 1.1 km window area centered on the segment was searched to identify the majority land cover type, both within and outside of the fire perimeter. The segment was labeled as being potentially influenced by this barrier if the majority of land cover outside a perimeter segment was one of these barrier types, and was assigned to be limited by this barrier only when there was a switch from another non-barrier type inside the adjacent burned area, i.e., when the percentage of the land cover barrier was less than 30% within the inside buffer and greater than 50% outside perimeter. The buffer was 500 m in width along each segment on both sides. For each individual fire, the total number of edge segments along the fire perimeter influenced by a particular barrier was divided by the total fire perimeter length to derive the percentage of fire edge affected.

The fire edge affected by fuels younger than 20 years old was analyzed using a similar approach as described above. An important criterion was that the percentage of young fuels outside the perimeter was greater by 30% than the percentage of young fuels inside the perimeter. Edge segments were considered influenced by roads or ridgelines if there were more than 500 m of road length within a 1.1 × 1.1 km window area centered on the segment.

In the case of overlapping categories of barriers, the attribution was assigned according to this order: non-flammable land cover, young stands, roads, and ridgelines. This was done to ensure mutually exclusive attribution. Fire growth along perimeter segments that were not associated with any of the above categories

(about 10–11%) was probably limited by weather, other existing fuel breaks, fire lines, and other factors not captured by the datasets used in our analysis. We calculated the effectiveness of each type of barrier as the percentage of their presence in the 1 km buffered area outside of the fire perimeter over their totals within fire affected and buffer areas.

2.4. Controls and regression models for structure loss

We examined the controls of human, biophysical, and meteorological variables on the spatial and temporal variability of both the probability and number of structures destroyed for the two types of fire. A total of 23 explanatory variables for individual fires equal to or greater than 40 ha (100 acres) during 1990–2009 were examined, including (a) fire size (FS) (log transformed); (b) 8 meteorology variables averaged over the fire perimeter area: RH, wind speed (log), Fosberg fire weather index (FFWI) (log) during the first two days of fire, preceding March–May precipitation, and two cumulative precipitation indices from the previous three winters and from the previous three water years, monthly RH and monthly vapor pressure deficit; (c) 3 topographical variables: mean slope, slope variance, and mean elevation within the fire perimeter; (d) 7 human variables: population, number and value of housing units (log transformed), mean road density within the fire perimeter, and distances to major, minor roads and housing; and (e) 4 vegetation variables: mean stand age and percent of stands less than 30 years within fire perimeter, as well as mean stand age and percent of stands equal to or less than 10 years at the edge of the 1 km buffer area outside of the fire perimeter.

We built empirical models to assess the probability of structure loss for individual fires using the sequential logistic regression method (*sequentialfs*) in Matlab. Stepwise regression was used to model and examine the controls on the number of structures destroyed for SA and non-SA fires. A similar stepwise regression was performed for the suppression cost per unit burned area and per fire perimeter length. We used the regression model for suppression cost to estimate suppression costs for fires during 1990–1994 when the record of suppression costs was not available from the USFS data record.

2.5. Future fire dynamics from climate change

We predicted how SA and non-SA fires will change in future climate, using the previously developed statistical meteorology-fire models that were optimized separately for the number and size of SA and non-SA fires at a monthly time scale during the historical period (Jin *et al* 2014). These separate regression models captured the influence of weather on fuel flammability, fuel drying, and wind-driven fire spread, and also the influence of previous cumulative precipitation as a proxy of fuel load and connectivity on the number of fires (figure S3). The 6 km resolution regional climate change signals were generated by downscaling 'present-day' (1981–2000) climate from NARR and 'future' (2041–2060) climate change signals, which were then added to the 1981–2000 NARR boundary forcing (Sun *et al* 2015, Walton *et al* 2015). The climate change signals were simulated by 5 global climate models under the RCP8.5 'business as usual' emission scenario and as reported in the Coupled Model Intercomparison Project Phase 5 archive on the Earth System Grid (Meinshausen *et al* 2011): CCSM4, CNRM-CM5, GFDL-CM3, MIROC-ESM-CHEM, and MPI-ESM-LR (Taylor *et al* 2012). The dynamical downscaling was performed with the Weather Research and Forecasting (WRF) model, version 3.2 (Skamarock *et al* 2011).

We also estimated the change in the number of structures destroyed by future SA and non-SA fires as a consequence of climate change, assuming the wildland urban interface remained unchanged. The probability of future structures destroyed was calculated with our regression models; the number of future properties destroyed was then calculated for those fires with a probability greater than 0.5, and then summarized over each month and for each fire type. Finally, the monthly probability-adjusted number of structure destroyed was scaled by the relative increase of number of fires to derive the future structure loss. We assumed that the spatial distribution and density of housing and population remained constant, and our analysis focused on the impact of future climate change. To account for the impact of FS increase on the number of structures or population at risk (H_{risk}), we built separate regression models, following the form $\ln(H_{\mathrm{risk}}) = a \cdot \ln^2(\mathrm{FS}) + b \cdot \ln(\mathrm{FS}) + c$, to relate the contemporary risk (H_{risk}) with the quadratic terms of log-transformed FS for SA and non-SA fires, respectively.

3. Results

3.1. Contrasting patterns of fire behavior

We used sequences of satellite images collected by NASA's MODIS during 2002–2009 (Giglio *et al* 2003) to determine the spread rate, duration, and intensity of SA and non-SA fires that were greater than 2500 ha and with 6 or more active fire counts detected. SA fires typically expanded to the west and northwest at high rates, as expected with strong offshore winds, whereas non-SA fires had slower spread rates and typically expanded to the east (figures 2(a), (b)). The mean spread rate of SA fires was $0.56 \pm 0.20\,\mathrm{km\,h^{-1}}$ along the major axis and $0.36 \pm 0.20\,\mathrm{km\,h^{-1}}$ along the minor axis; these rates were more than twice those of non-SA fires ($p < 0.001$; $n = 30$ and 26). Both SA and non-SA fires spread most rapidly around midday, with SA fires consuming $1094 \pm 564\,\mathrm{ha\,h^{-1}}$ and non-SA

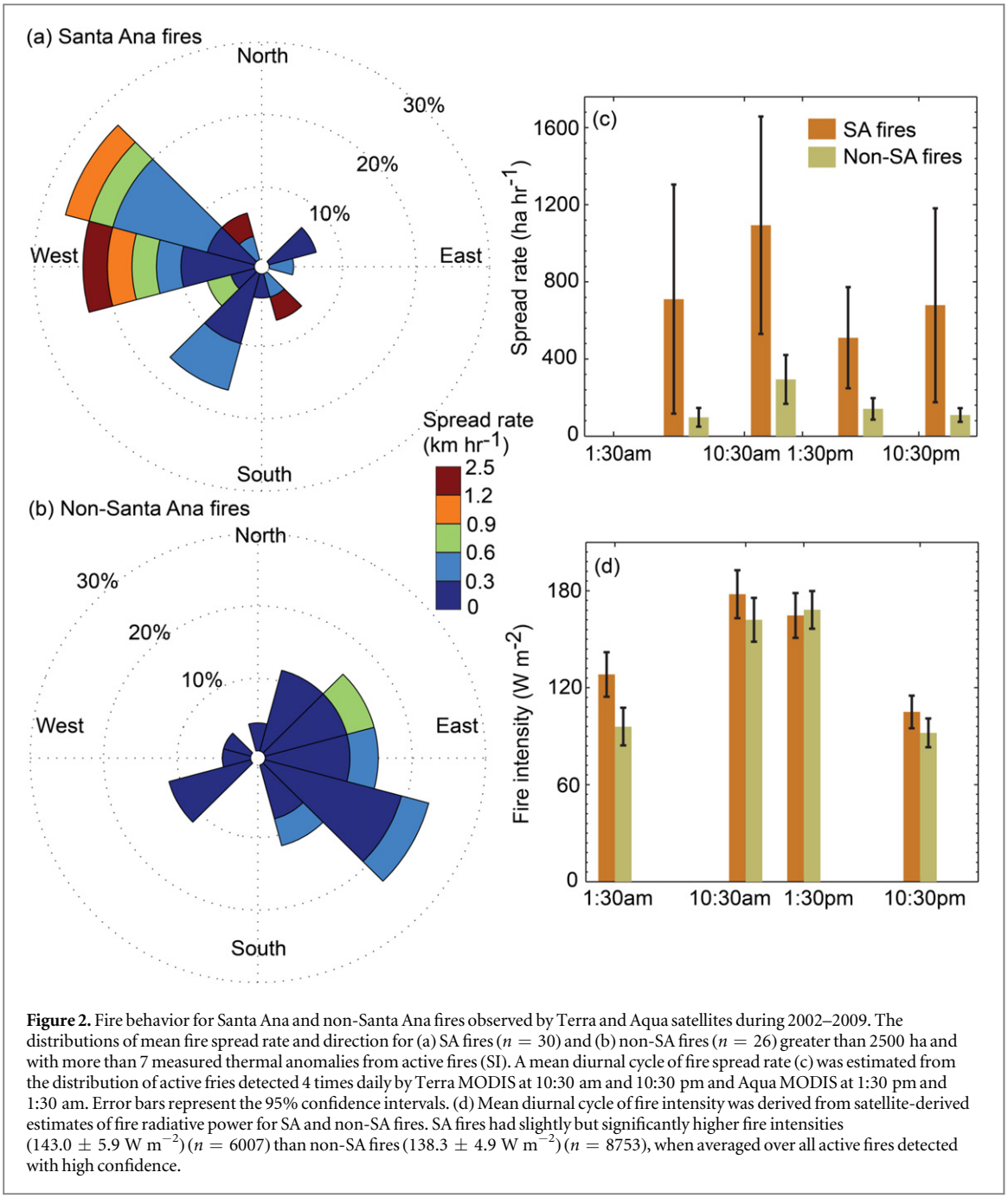

Figure 2. Fire behavior for Santa Ana and non-Santa Ana fires observed by Terra and Aqua satellites during 2002–2009. The distributions of mean fire spread rate and direction for (a) SA fires ($n = 30$) and (b) non-SA fires ($n = 26$) greater than 2500 ha and with more than 7 measured thermal anomalies from active fires (SI). A mean diurnal cycle of fire spread rate (c) was estimated from the distribution of active fries detected 4 times daily by Terra MODIS at 10:30 am and 10:30 pm and Aqua MODIS at 1:30 pm and 1:30 am. Error bars represent the 95% confidence intervals. (d) Mean diurnal cycle of fire intensity was derived from satellite-derived estimates of fire radiative power for SA and non-SA fires. SA fires had slightly but significantly higher fire intensities (143.0 ± 5.9 W m^{-2}) ($n = 6007$) than non-SA fires (138.3 ± 4.9 W m^{-2}) ($n = 8753$), when averaged over all active fires detected with high confidence.

fires 295 ± 127 ha h^{-1} (figure 2(c)). SA fires lasted 4.9 ± 2.5 days on average, and often consumed half of the final burn area within the first day. Non-SA fires lasted longer (13.0 ± 9.7 days), and consumed only 20% of the final area during the first two days. SA fires were more intense than non-SA fires, especially at night (116 ± 8 versus 94 ± 7 W m^{-2}) (figure 2(d)).

3.2. Contrasting fuel controls on fire

SA fire probability was not correlated with stand age; about 1% of the undeveloped area in each age class burned annually in SA fires (figure 3(a)). In contrast, non-SA fire probability significantly increased with age from 0.7 ± 0.2% for stands younger than 20 years to 1.5 ± 0.8% for the 40–60 year and 60 year plus classes. We calculated the mean age distribution within the areas burned for SA and non-SA fires greater than 100 acres, and within the 1 km buffered areas outside of fire perimeters, separately. Only a slightly higher (and non-significant) percentage of young fuels were found outside of SA fire perimeters. In contrast, a statistically significant higher percentage of ecosystems with stands younger than 20 years was found outside of the non-SA fire perimeters. These results indicated that stand age plays a more important role in limiting the growth of non-SA than SA fire.

We investigated the spatial correspondence between final burn perimeter and barriers such as non-flammable land cover, recent burns, roads, and ridgelines. About 64% of SA and 54% of non-SA

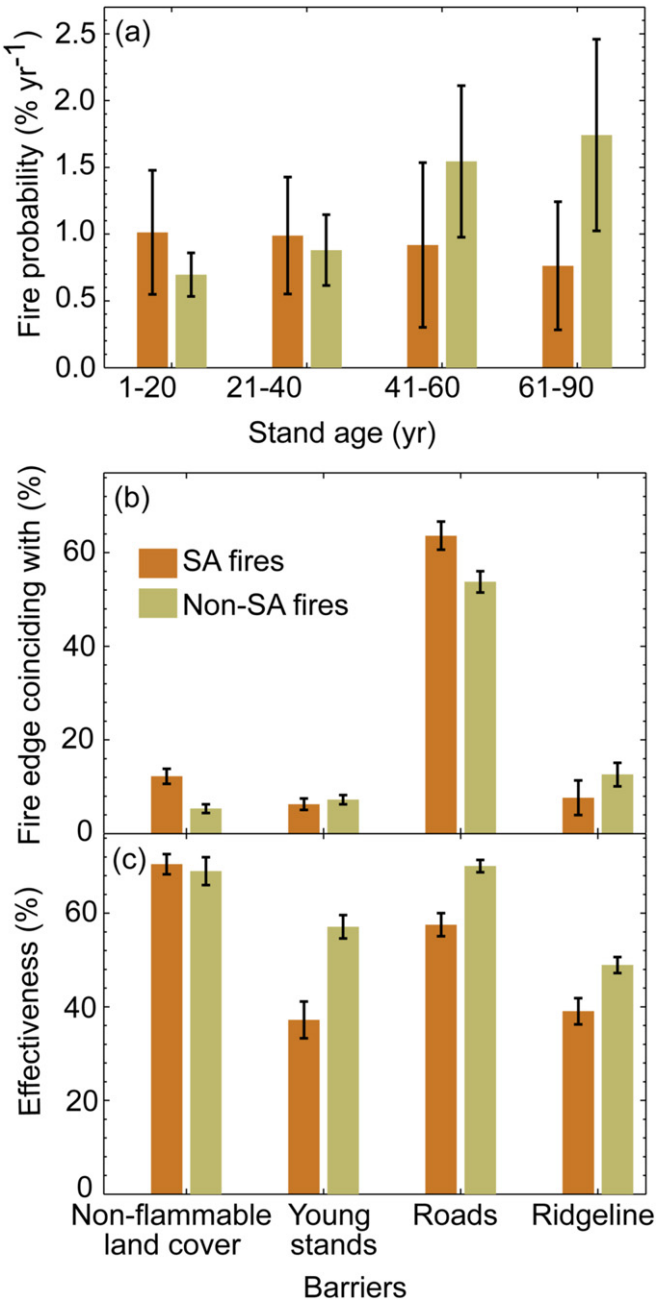

Figure 3. Effects of stand age and fuel breaks on fire probability. In panel (a), fire probability was calculated as the percent of area burned for each age group over the total available vegetated land area for the same age group in each year during 1959–2009. Panel (b) shows the percentage of fire perimeter length affected by non-flammable land cover types, stands 20 years or younger, roads, and ridgelines. Non-flammable land cover types included urban, agriculture, and ocean/lake, and additionally deserts and high elevation barren areas for non-SA fires. The effectiveness of a potential barrier (c) was calculated as the percentage of its presence in the 1 km buffered area outside of the fire perimeter over the total within fire-affected and buffered areas.

perimeters coincided with existing roads; these roads presumably acted as fuel breaks and facilitated access for suppression (Narayanaraj and Wimberly 2011). Another 12% of SA and 5% of non-SA perimeters were located in interface areas between wildland and non-flammable land cover, such as urban, agriculture, water, or barren (figure 3(b)). Areas in transitions along the perimeter from older stands to ones that burned within the last 20 years accounted for 6−7% of the perimeter of both fire types. Ridgelines, which provide a favorable location for constructing fire breaks (National Wildfire Coordinating Group 1996), accounted for 8% of SA and 13% of non-SA perimeters. Roads were slightly more effective at limiting the spread of non-SA fires; approximately 72% of the road length within a burned area created a barrier to additional non-SA fire growth, compared with 56% for SA fires. Likewise, younger stands and ridgelines were significantly more effective at stopping the spread of non-SA fires than SA fires (figure 3(c)).

Table 1. Socio-economic impacts of Santa Ana (SA) and non-Santa Ana (non-SA) fires.

Annual fires and impacts[a] (per year)	All fires		Fires > =5000 ha	
	SA	non-SA	SA	non-SA
Number of fires (> = 100 acres)	9.8	32.1	1.7	1.6
Burned area (10^3 ha)	37.2	41.4	31.2	27.8
Structures at risk	3409.2	439.6	2832.0	139.1
Population at risk	9073.1	1085.8	7631.4	325.8
Housing value at risk (M$)	1015.5	142.6	808.3	22.1
Structures destroyed	515.8	112.0	422.7	48.5
Structures damaged	68.5	7.5	37.6	4.6
Fatalities (fire personnel)	0.5	0.4	0.4	0.2
Fatalities (civilian)	1.6	0.1	1.4	0.1
Fires with damages: number	3.2	3.4	1.3	0.9
Fires with damages: area (10^3 ha)	29.7	24.9	26.7	21.6
Housing value destroyed (M$)	156.4	38.5	118.3	6.7
Suppression cost[b] (M$)	29.5	63.0	17.8	32.1
Impacts (per fire or burned area)				
Housing value destroyed (M$ per fire)	16.0	1.2	71.7	4.2
Suppression cost[b] (M$ per fire)	6.7 ± 2.2	6.3 ± 3.1	18.0 ± 5.2	28.8 ± 16.6
Housing value destroyed ($ per ha)	4203.2	928.2	3786.1	239.9
Suppression cost[b] ($ per ha)	600.2	1040.4	460.2	965.1

[a] The population and structures at risk within each individual fire polygon during 1990–2009 were calculated based on the 2000 US. Census Bureau's block and block-group data. The population at risk was estimated as the number of people living within the boundaries of the final fire perimeter.

[b] Fire expenditures were assembled and summarized for fires available during 1995–2009. A regression analysis (SI text) was done to extrapolate expenditure data record to 1990–2009.

3.3. Patterns of structure loss and fatalities

SA fires often encroached into densely populated coastal areas, putting a large number of structures at risk (figure 1, table 1). SA fires affected more than 9000 people and threatened more than 3400 structures in an average year, with a cumulative value of at least $20 billion during 1990–2009. By contrast, non-SA fires typically occurred in sparsely populated inland areas, resulting in impacts for these indicators that were typically about 7 to 8 fold lower than those for SA fires, even though both types of fire burned similar total areas. Civilian fatalities and the number of structures destroyed or damaged followed similar patterns, with the impact of SA fires far exceeding that of non-SA fires. Fires over 5000 ha accounted for a disproportionate fraction of total damage and risk for both SA and non-SA fires. The 33 largest SA fires out of a total of 196 accounted for more than 80% of total fatalities and structures destroyed during 1990–2009. Similarly, the 32 largest non-SA fires out of 642 accounted for over 43% of structures destroyed.

For the binary prediction of the properties destroyed, the sequential logistic model for both SA and non-SA fires had a prediction accuracy of about 68%, calculated as a ratio of number of fires that were predicted correctly with an assignment of 'yes' or 'no' for structures destroyed relative to the total number of fires. Housing at risk, RH, FS, distance to minor road, and population at risk were significant explanatory variables, and no variables related to stand age was significant in explaining if there were structures destroyed for SA fires ($n = 151$). For non-SA fires ($n = 411$), increasing FS and FFWI increased the possibility of structures being destroyed; reduced precipitation during a couple of consecutive years and older stands within the area burned also promoted the likelihood of structure loss.

We log-transformed the total number of the structures destroyed, and regressed it against various environmental drivers using a stepwise regression method for all fires with structures destroyed. The total number of houses at risk within the fire perimeters was the most significant variable for both fire types, explaining 47% of variance in the number of structures destroyed by SA fires and 25% by non-SA fires (table 2). Distance to minor roads explained additional 7% for SA fires, with fires occurring further away from roads having more structures destroyed, probably as a consequence of difficulty of access for initial suppression. FFWI and elevation explained another 12% and 7% for non-SA fires.

3.4. Fire suppression expenditures

Money spent fighting an average SA fire during 1995–2009 ($6.7 ± 2.2 M) was roughly the same as that spent for a non-SA fire ($6.3 ± 3.1 M) (table 1). The expenditures per area burned were considerably lower for SA fires ($792 per ha) than for non-SA fires ($1522 per ha). Similarly, the cumulative amount spent fighting SA fires during 1995–2009 ($390 M)

Table 2. Variables affecting the number of structures destroyed (log-transformed) by individual fires during 1990–2009, based on the stepwise regression analysis.

ln (number of structures destroyed)		Coefficient	SE	pval	cumu R^2	RMSE	Intercept
Santa Ana fires ($n = 62$)							0.072
	ln (housing at risk)	2.4460	0.7669	0.003	0.47	1.6	
	Distance to minor roads	2.3723	0.9753	0.019	0.54	1.5	
	ln (population at risk)	−1.7839	0.7467	0.021	0.59	1.4	
Non Santa Ana fires ($n = 66$)							−2.420
	ln (housing at risk)	0.4500	0.0715	0.000	0.25	1.4	
	ln (FFWI)	1.0023	0.3981	0.010	0.37	1.3	
	Elevation (m)	0.0013	0.0005	0.007	0.44	1.2	
	Preceding winter and spring precipitation (mm)	−0.0024	0.0012	0.044	0.49	1.2	

was well below that spent on non-SA fires ($743 M). These patterns were amplified for the largest fires, where expenditures for a SA fire ($13.7 ± 4.2 M per fire) were significantly lower than for a non-SA fire ($22.2 ± 11.4 M). The suppression investment per housing value destroyed was ten times greater for non-SA fires than for SA fires (table 1), although fire suppression efforts are influenced by a range of objectives, many of which are unrelated to protection of housing value.

The westward expansion towards the urbanized coastal zone, faster rate of fire spread, and greater intensity of SA fires were probably the main drivers of the disproportionate economic impact of this fire type, whereas the longer duration of non-SA fires likely increased suppression costs. The rapid growth and short duration of SA fires may limit opportunities to deploy resources that might prevent damage, and explains, in part, why suppression costs were relatively low for this fire type.

3.5. Future projections with climate change

Separate regression models were built to predict fire occurrence and size as a function of meteorology using contemporary time series of meteorology and fires as shown in Jin *et al* (2014) (figure S3). Here we forced these models with climate projections for the mid-21st century that were created by dynamically downscaling output from five climate model simulations for the representative concentration pathway 8.5 (RCP8.5) (figure S4). The combined models predicted shifts in fire number, size and total area burned for both SA and non-SA fires (figures 4 and S5). Four of the five climate models predicted more intense SA events, which are expected to increase SA FS, mostly by reducing RH and secondly by increasing wind speed (figures S5 and S6). The overall area burned by SA fires increased 64% on average (95% CI: −12%–140%) by 2041–2060 relative to 1981–2000.

In parallel, the area burned by non-SA fires in May–September was estimated to increase by 77% (95% confidence intervals (CI) of 32% − 121%; figure 4). The increase in non-SA burn area was mainly driven by increases in FS with a warmer and drier climate. All five climate models predicted strong warming under the RCP8.5 scenario, especially in summer, with 2–4 °C warming in August (figure S4). Shifts in precipitation also influenced the projections of non-SA fires in our statistical climate-fire model, likely by controlling fine fuel amount and fuel connectivity from locations such as roads to areas with dense fuel (Jin *et al* 2014). CNRM-CM5, one of the CMIP5 models, projected significant increases in wet season precipitation, which contributes to an increase in the number of non-SA fires in this projection (figures 4, S5 and S6). The other four climate models predicted reduced wet season precipitation, which presumably decreased fuel load and connectivity and thus counteracted the impacts of summer warming for the number of non-SA fires (Figure S6).

To predict the number of structures and population at risk as a consequence of FS increases in the future, we built the regression models using the quadratic terms as described in section 2.5. For SA fires, the housing and population at risk typically scales well with FS, and when structures (or population) at risk and FS were log transformed, the correlation coefficient was 0.66 ($p < 0.0001$). The dependence of structures and population at risk on FS was less significant for non-SA fires, with correlation coefficients of 0.37 ($p < 0.0001$) between the log-transformed structures at risk and FS and 0.30 ($p < 0.0001$) for FS and the log transformed population at risk. Climate-induced changes in SA fires by 2041–2060 were estimated to increase the number of structures destroyed by 20% (±7%) on average based on the stepwise regression model we developed here, assuming all other conditions remain constant. The number of structures destroyed by non-SA fires was estimated to increase by 74% (±56%). The probability of structure loss was estimated to increase by 92% (±23%) for an average SA fire, and by 65% (±57%) for a non-SA fire, primarily as a consequence of the projected increases in FS.

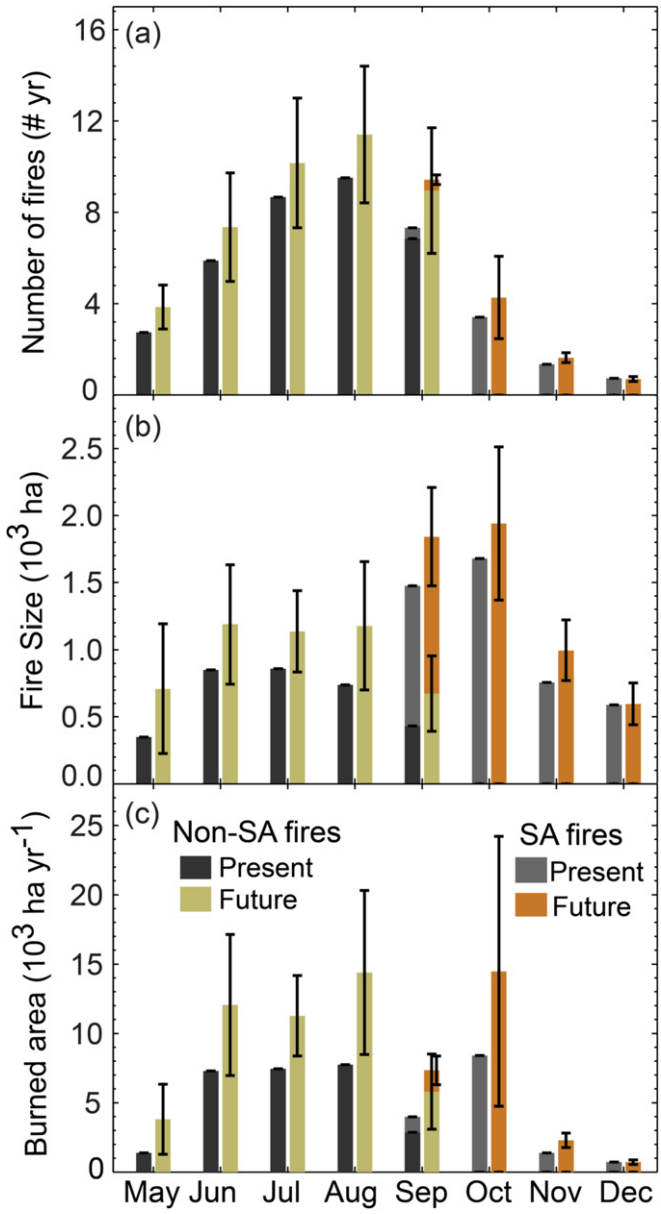

Figure 4. The response of SA and non-SA fires to climate change during the middle part of the 21st century for the RCP8.5 scenario. Separate meteorology-fire models for SA and non-SA fires were optimized from 59 years of fire history and 6 km climate output from a regional climate model constrained by reanalysis observations. High resolution present (1980–2000) and future (2040–2060) climate, including Santa Ana frequency and intensity, was derived from dynamic downscaling of the NARR reanalysis data and 5 global climate model simulations with the Weather Research and Forecasting (WRF) model.

4. Discussion and implications

Separation of Southern California wildfires into SA and non-SA components using high resolution meteorology creates a framework for better understanding Southern California's contemporary and future fire regime (Jin *et al* 2014). This partitioning resolves some of the long-standing debate over the relative importance of meteorology and fuels in controlling the spread of Californian wildfires (Minnich 1983, Keeley *et al* 1999). Meteorology was clearly the dominant factor controlling SA fires; the spatial and temporal variability of SA FS was well correlated with meteorological drivers, including RH and wind as modulated by terrain (see also figure S3). This finding is consistent with past work showing the probability of burned area in high wind corridors is elevated compared to other areas (Moritz *et al* 2010). SA fire probability did not depend on stand age, and we did not find evidence that age-dependent flammability limits SA fire spread, contrary to the fine-grain age patch model (Minnich and Chou 1997). On the other hand, fuels played a comparatively important role in controlling non-SA fires. We found a positive relationship between fire probability and stand age in areas affected by non-SA fires. Additionally, younger stands were a more effective barrier to the growth of non-SA fires, and the mean age within large non-SA fires was comparatively older than that of smaller fires (table S1). These results have implications for management

and the likely efficacy of strategies to reduce fuels, including the use of prescribed fire. Our results suggest fuel abatement strategies are more likely to succeed in areas dominated by non-SA fires because these fires were found to be more sensitive to variations in stand age, and stand age is known to be a primary driver of fuel amount and composition (Barbour and Billings 2000). The effectiveness of fuel treatments also are likely evolving a consequence of climate-induced changes in fire weather, and thus an adaptive approach is needed for evaluating the success of these investments.

Our economic analysis of SA and non-SA fires raises, but does not resolve, the issue of whether current firefighting resources are allocated optimally by fire type. We found that SA fires placed considerably more structures and human lives at risk (with more than 7 fold higher impacts than non-SA fires), whereas suppression expenditures were slightly lower for this fire type. While this may appear to argue for investing more resources into SA fire suppression, we lack the information to evaluate whether additional investments would yield measureable benefits. In particular, more information is needed on how FS and damages are controlled by prevention and suppression expenditures, and on the marginal benefit that would accrue with increased resources by fire type (US Goverment Accoutability Office 2007). For example, it is possible that an increase in allocation to SA fire suppression would have little benefit (Safford 2007), given the strong meteorological control we found for these fires, as well as the short time interval between ignition and struture loss. The identification and characterization of fire impacts by type raises the possibility of an improved allocation of resources, but a better understanding of the effectiveness and potential benefits of fire management strategies is needed to determine whether a shift in allocation is justified (Department of the Interior 2012, Gebert and Black 2012, Houtman *et al* 2013, Thompson *et al* 2013).

Recognition of the two different fire types in Southern California also carries implications for efforts to predict and prepare for future changes. Our analysis indicated changes in Southern California's fire regime with climate change will be greatest for non-SA fires. The two types of fire are spatially and temporally distinct, and the controlling climate factors diverge (Jin *et al* 2014), suggesting that an increase in non-SA fires carries different implications from what would be expected for SA fires. Non-SA fires occur primarily during summer, which may increase competition with other regions for firefighting resources as fire activity throughout the western US is expected to increase during this season (Westerling *et al* 2003, McKibben 2014). Summer fires may contribute to interactions between heat and air quality, exacerbating climate-driven health risks across the western US (Kinney 2008, Buckley *et al* 2014). Non-SA fires are concentrated inland, often at higher elevations (table S1), and cause significant tree mortality in montane forests. Semi-arid forests in the southwestern US are already prone to catastrophic crown fire as a legacy of fire suppression since the beginning of the 20th century and subsequent fuel accumulation (Hurteau *et al* 2013, Safford and van de Water 2014, Taylor *et al* 2014). Increasing incidence of summer fire will likely amplify this risk and may increase the chance of an upslope shift in vegetation distribution and type conversion from montane forest to shrubland at higher elevations (Nagel and Taylor 2005, Kelly and Goulden 2008), with implications for the goods and services provided by these ecosystems.

The statistical climate-fire models developed and used for future fire projection here did not include stand age as a dependent variable, and thus were not able to resolve a possible negative feedback from fuel–fire interactions. We recognize that there would be less fuels available as fire frequency increases in the future, especially in the case of non-SA fires, which may limit the fire activity, especially at the later part of mid-21 century. Our models considered the impact of precipitation change on fires, presumably by regulating fuel amount and connectivity. A fully coupled dynamic vegetation model simulation is needed to further understand the climate-fuel feedback and the co-evolution of the landscape and fire risk. Predicting future housing density and its spatial pattern is also a critical next step for understanding economic losses associated with SA fires.

The SA wind events studied here are examples as dry and hot Foehn winds; these winds occur in the lee-side of the mountain ranges and are associated with the elevated fire danger in many other parts of the world, including Europe and Australia (Sharples *et al* 2010). Thus, the meteorological downscaling and fire partitioning approaches developed here may enable more quantitative assessments of economic impact and future change in other regions. Within Southern California and the Western US, an important next step is to integrate risks from changing wildland fires with information on other climate change impacts to more effectively design management solutions that preserve diversity, ecosystem function, and services.

Acknowledgments

This research was supported by NASA grant NNX10AL14G and the Jenkins Family Foundation. We are also grateful to Dr H Safford for his comments and Drs K Gebert and D Sapsis for their help with acquiring and interpreting the economic data.

References

Barbour M G and Billings W D 2000 *North American Terrestrial Vegetation* (Cambridge: Cambridge University Press)

Batllori E, Parisien M A, Krawchuk M A and Moritz M A 2013 Climate change-induced shifts in fire for Mediterranean ecosystems *Glob. Ecol. Biogeogr.* **22** 1118–29
Buckley J P, Samet J M and Richardson D B 2014 Does air pollution confound studies of temperature? *Epidemiology* **25** 242–5
California Department of Foresty and Fire Protection 2013 *Fire and Resource Assessment Program (FRAP) Fire Perimeter Data* California Department of Foresty and Fire Protection
Conard S G and Weise D R (ed) 1998 Management of fire regime, fuels, and fire effects in southern California Chaparral: lessons from the past and thoughts for the future *Fire in Ecosystem Management: Shifting the Paradigm From Suppression to Presciption (Tall Timbers Fire Ecology Conf. Proc. (Tallahassee, FL))* pp 342–50
Daly C, Halbleib M, Smith J I, Gibson W P, Doggett M K, Taylor G H, Curtis J and Pasteris P P 2008 Physiographically sensitive mapping of climatological temperature and precipitation across the conterminous United States *Int. J. Climatol.* **28** 2031–64
Department of the Interior 2012 *Wildland Fire Management Program Benefit-Cost Analysis: A Review of Relevant Literature* Department of the Interior, Office of Policy Analysis
Gebert K M and Black A E 2012 Effect of suppression strategies on federal wildland fire expenditures *J. Forest* **110** 65–73
Gebert K M, Calkin D E and Yoder J 2007 Estimating suppression expenditures for individual large wildland fires *West. J. Appl. For.* **22** 188–96
Giglio L, Descloitres J, Justice C O and Kaufman Y J 2003 An enhanced contextual fire detection algorithm for MODIS *Remote Sens. Environ.* **87** 273–82
Giglio L, Loboda T, Roy D P, Quayle B and Justice C O 2009 An active-fire based burned area mapping algorithm for the MODIS sensor *Remote Sens. Environ.* **113** 408–20
Giglio L, Randerson J T and van der Werf G R 2013 Analysis of daily, monthly, and annual burned area using the fourth-generation global fire emissions database (GFED4) *J. Geophys. Res.—Biogeo.* **118** 317–28
Houtman R M, Montgomery C A, Gagnon A R, Calkin D E, Dietterich T G, McGregor S and Crowley M 2013 Allowing a wildfire to burn: estimating the effect on future fire suppression costs *Int. J. Wildland Fire* **22** 871–82
Hughes M and Hall A 2010 Local and synoptic mechanisms causing Southern California's Santa Ana winds *Clim. Dyn.* **34** 847–57
Hurteau M D, Bradford J B, Fule P Z, Taylor A H and Martin K L 2013 Climate change, fire management, and ecological services in the southwestern US *Forest Ecol. Manag.* **327** 280–9
Jin Y F, Randerson J T, Faivre N, Capps S, Hall A and Goulden M L 2014 Contrasting controls on wildland fires in Southern California during periods with and without Santa Ana winds *J. Geophys. Res.—Biogeo.* **119** 432–50
Keeley J E, Fotheringham C J and Morais M 1999 Reexamining fire suppression impacts on brushland fire regimes *Science* **284** 1829–32
Keeley J E, Safford H, Fotheringham C J, Franklin J and Moritz M 2009 The 2007 Southern California wildfires: lessons in complexity *J. Forest* **107** 287–96
Kelly A E and Goulden M L 2008 Rapid shifts in plant distribution with recent climate change *Proc. Natl Acad. Sci. USA* **105** 11823–6
Kinney P L 2008 Climate change, air quality, and human health *Am. J. Prev. Med.* **35** 459–67
McKibben B 2014 Climate change impacts in the United States: the third national climate assessment *New York Rev. Books* **61** 46–8
Meinshausen M *et al* 2011 The RCP greenhouse gas concentrations and their extensions from 1765 to 2300 *Clim. Change* **109** 213–41
Mesinger F *et al* 2006 North American regional reanalysis *Bull. Am. Meteorol. Soc.* **87** 343
Minnich R A 1983 Fire mosaics in Southern-California and Northern Baja California *Science* **219** 1287–94
Minnich R A and Chou Y H 1997 Wildland fire patch dynamics in the chaparral of southern California and northern Baja California *Int. J. Wildland Fire* **7** 221–48
Moritz M A, Moody T J, Krawchuk M A, Hughes M and Hall A 2010 Spatial variation in extreme winds predicts large wildfire locations in chaparral ecosystems *Geophys. Res. Lett.* **37** L04801
Nagel T A and Taylor A H 2005 Fire and persistence of montane chaparral in mixed conifer forest landscapes in the northern Sierra Nevada, Lake Tahoe Basin, California, USA *J. Torrey Bot. Soc.* **132** 442–57
Narayanaraj G and Wimberly M C 2011 Influences of forest roads on the spatial pattern of wildfire boundaries *Int. J. Wildland Fire* **20** 792–803
National Wildfire Coordinating Group 1996 *Wildland Fire Suppression Tactics Reference Guide* NFES 1256, Boise, ID: National Interagency Fire Center
Safford H D 2007 Man and fire in Southern California: doing the math *Fremontia* **35** 25–9
Safford H D and van de Water K M 2014 Using fire return interval departure (FRID) analysis to map spatial and temporal changes in fire frequency on national forest lands in California *Research Paper* PSW-RP-266 USDA Forest Service, Pacific Southwest Research Station
Sharples J J, Mills G A, Mcrae R H D and Weber R O 2010 Foehn-like winds and elevated fire danger conditions in southeastern Australia *J. Appl. Meteorol. Clim.* **49** 1067–95
Skamarock W C, Klemp J B, Dudhia J, Gill D O, Barker D M, Guda M G, X-Y H, Wang W and Powers J G 2011 A description of the Advanced Research WRF version 3 *NCAR Technical Note* NCAR
Sun F, Walton D and Hall A 2015 A hybrid dynamical–statistical downscaling technique, part II: end-of-century warming projections predict a new climate state in the Los Angeles region *J. Climate* **28** 4618–36
Taylor A H, Vandervlugt A M, Maxwell R S, Beaty R M, Airey C and Skinner C N 2014 Changes in forest structure, fuels and potential fire behaviour since 1873 in the Lake Tahoe Basin, USA *Appl. Veg. Sci.* **17** 17–31
Taylor K E, Stouffer R J and Meehl G A 2012 An Overview of CMIP5 and the experiment design *Bull. Am. Meteorol. Soc.* **93** 485–98
Thompson M P, Calkin D E, Finney M A, Gebert K M and Hand M S 2013 A risk-based approach to wildland fire budgetary planning *Forest Sci.* **59** 63–77
Uppala S M *et al* 2005 The ERA-40 re-analysis *Q. J. R. Meteorol. Soc.* **131** 2961–3012
US Goverment Accoutability Office 2007 *Wildland Fire Management: Lack of Clear Goals or a Strategy Hinders Federal Agencies' Efforts to Contain the Costs of Fighting Fires* United States Goverment Accoutability Office
Walton D, Sun F and Hall A 2015 A hybrid dynamical–statistical downscaling technique, part I: development and validation of the technique *J. Climate* **28** 4597–617
Westerling A L and Bryant B P 2008 Climate change and wildfire in California *Clim. Change* **87** S231–49
Westerling A L, Bryant B P, Preisler H K, Holmes T P, Hidalgo H G, Das T and Shrestha S R 2011 Climate change and growth scenarios for California wildfire *Clim. Change* **109** 445–63
Westerling A L, Gershunov A, Brown T J, Cayan D R and Dettinger M D 2003 Climate and wildfire in the western United States *Bull. Am. Meteorol. Soc.* **84** 595
Westerling A L, Hidalgo H G, Cayan D R and Swetnam T W 2006 Warming and earlier spring increase western US forest wildfire activity *Science* **313** 940–3